Title: An analysis of the immune compartment within bovine adipose tissue.

Authors: Eleanor G Bentley, Glesni Pugh, Laura Gledhill and Robin J Flynn*

Address: Department of Infection Biology, Institute of Infection and Global Health, University of Liverpool, L3 5RF

Corresponding Author: Dr Robin J Flynn; rjflynn@liverpool.ac.uk

Keywords: bovine; leukocyte; eosinophil; adipose; mesenteric

Running title: Leukocytes in bovine adipose tissue

Abstract

Adipose tissue (AT) has wide functions as an active endocrine organ acting as a site of nutrient storage and thermogenesis. Recently it has been identified as having a key role in murine and human immunity and inflammation. Type 1 or type 2 immune responses and their respective cytokines have been linked to white or brown AT, respectively. Most dramatic is the involvement of type-2 innate lymphoid cells (ILC2s) in stimulating eosinophil recruitment via interleukin (IL)-13 which in turn stimulates alternative macrophage activation via IL-4/IL-13. Recruited leukocytes are capable of influencing the cellular composition and function of adipose tissue and present a route to combat human obesity, however these processes are poorly understood in ruminants. Here we have characterised the resident leukocytes populations within bovine mesenteric AT (MAT) and subcutaneous AT (SAT), compared with the corresponding mesenteric lymph node (MLN). Concurring with related studies, we find bovine AT has its own resident leukocyte populations where eosinophils and neutrophils dominate. Importantly the proportion of eosinophils or neutrophils corresponded to the adipocyte size found in both depots. Further exploration of this area may have important implications on the food production industry or could be applied to improve the course of pathogenesis during disease.

1. Introduction

Until recently adipose tissue was considered metabolically unremarkable, functional only in triglyceride storage and non-shivering thermogenesis (Cannon and Nedergaard, 2004). Studies attempting to treat obesity led to a greater understanding of the composition and function of adipose tissue; now adipose tissue is widely accepted as an active endocrine organ, capable of manipulating both metabolic and inflammatory pathways through adipokine secretion (Lehr, Hartwig and Sell, 2011). The most surprising relationship to arise from these studies is an understanding of the resident leukocyte populations and how these interact with adipocytes and how readily one can shape the other through alterations in signalling or cellular composition.

Environmental adaptation to the cold triggers a norepinephrine signalling cascade from the hypothalamus to stimulate a brown adipose tissue (BAT) associated expression profile, including peroxisome proliferator-activated receptor γ (PPARγ) and uncoupling-protein 1 (UCP1), instigating thermogenesis (Nguyen et al., 2011; Johnson et al., 1977). This pathway has been found to be dependent on leukocyte involvement, mainly recruitment of ILC2s mediated by IL-33. The type 2 cytokines, IL-5 and IL-13, released by ILC2s mobilise eosinophils to the area; these in turn produce IL-4 (Lee et al., 2015) causing macrophage recruitment and alternative activation. Alternatively activated macrophage (AAM) produce norepinephrine in turn stimulating the beiging of adipocytes (Qiu et al., 2014). Nguyen et al. (2011) demonstrateded this pathway was essential when inducing cold conditions in *Il4*$^{-/-}$*Il13*$^{-/-}$ mice, where no macrophage migration to white adipose tissue (WAT) or BAT occurred, thereby severely impairing thermogenic adaptation. This mechanism is fundamental in initiating the

first non-shivering thermogenesis: IL-33 triggers the induction of UCP1 upon parturition, absence of IL-33 or its receptor ST2, impairs UCP1 expression despite the presence of normally developed BAT (Odegaard et al., 2016).

Research has looked to the manipulation of leukocytes to overcome adipose tissue deposition and has linked the inflammatory phenotype of leukocytes to human obesity. Preventing alternative activation of macrophages by PPARγ deletion was sufficient to render mice susceptible to glucose intolerance and obesity (Odegaardet al., 2007). PPARγ expresson is induced in macrophages by eosinophil derived IL-4, therefore maintenance of high eosinophil counts in adipose tissue may be essential in controlling obesity and glucose tolerance (Wu et al., 2011). Instinctive dietary control may already rely on this mechanism; Nussbaum et al. (2013) showed resident gastric ILC2 increase IL-5 and IL-13 production post feeding thereby stimulating eosinophilia.

Adipose tissue is known to be vital to the immune response to bacteria in insects (Azeez, Meintjes and Chamunorwa, 2014). A similar role is possible in mammals as key cytokines associated with adipose tissue are also associated with anti-parasitic immunity. IL-33 responsive ILC2s are particularly prevalent in mesenteric lymph node, spleen and liver, and are the key IL-13 expressing cells during helminth infection (Neill et al., 2010). ILC2s were found to rely on adipose tissue acid metabolism in mice when nutrient deprived and nematode challenged, where they selectively maintained IL-13 production over energy conservation; thus highlighting the balance between the two compartments (Wilhelm et al., 2016). ILC2s are core to the maintenance of IL-13 production as depletion of ILC2s dramatically impairs expansion of adipose tissue eosinophils even upon parasitic challenge

(Molofsky et al., 2013). Some parasites have been found to alter the somatic composition of adipose tissue – *Neospora caninum* tachyzoites residing in adipose tissue induce a strong local Th1 response and systemic leptin levels (Teixeira et al., 2015). Increased leptin due to leptin resistance would lead to increased adiposity therefore re-enforcing the local protective Th1 response within this tissue. .

Greater understanding of the interaction between adipose tissue and immune function could be fundamental in preventing or treating infection particularly in production animals where subclinical and chronic infection leads to enormous losses. However very little work has been done on ruminant adipose tissue. Smith et al. (2004) demonstrated variation in calf lipid store exhaustion times between breeds of cow, suggesting diversity in post-partum vulnerability to infection as a result of resource availability. In sheep at 12h post-parturition adipose tissue depots are depleted but UCP1 levels are found to peak. By 30 days post-parturition, UCP1 is almost undetectable indicating low BAT levels (Pope, Budge and Symonds, 2013). This may suggestive of a mechanism mobilised to combat the effects of peri-parturition nematode egg increases. Thus, maintaining BAT levels by stimulating UCP1 could improve immune function or even carcass composition of the animal.

To investigate if this was possible in cattle we sought toto assess what if any leukocyte population was present in the adipose tissue. To this end we characterised the immune profile, cellular composition and cytokine capacity, of bovine subcutaneous adipose tissue (SAT) and mesenteric adipose tissue (MAT), in contrast to the mesenteric lymph node (MLN). The same adipose sites were examined to determine the phenotype of adipocytes present and if this was related to the local leukocyte composition.

2. Methods

2.1 Sample collection

MLN, MAT and SAT were harvested from 10 clinically healthy beef cows at slaughter. Tissues were collected at two local premises (CH62 1AB) or (WN3 6PH). Animals were euthanised by standard application of captive bolt stunning and exsanguination. Samples were collected into sterile PBS for transport prior to processing. All animals sampled were male between the age of 14-18 months of age with a body condition score of 5-7.

2.2 Leukocyte and adipocyte preparations

MLN samples were pushed through a 100 μm cell strainer using a 5ml syringe then washed with PBS. The cell suspension was centrifuged at 500x*g* for 10 minutes, the supernatant removed and then the pellet resuspended in PBS and kept at 4 °C. Leukocytes were isolated from SAT and MAT by collagenase digestion as described in Cho, Morris and Lumeng (2014). In brief, adipose samples were minced in 1 mg/ml collagenase D (from *Clostridium histolyticum*) per gram of tissue, then incubated at 37 °C for 45 minutes. The solution was passed through a 100 μm cell strainer before centrifugation at 500x*g* for 10 minutes at 4 °C. Primary adipocytes were removed from the upper phase of the supernatant and the leukocytes pellet was resuspended in PBS. Residual adipocytes bound to the cell strainer were collected in PBS warmed to 37 °C, and added to the adipocyte fraction from the supernatant.

2.3 Total cell counts

Leukocytes were stained with trypan blue and viable cells counted in a haemocytometer by microscopy (CK, Olympus, Tokyo). Total cell counts were expressed per gram of tissue. The

144 cell suspension was centrifuged at 500x*g* for 10 minutes then resuspended in PBS to $1x10^6$
145 cells/mL. Cells were stored at 4 °C until use.

146 2.4 Differential cell count

147 Cytospins were prepared from leukocyte preparations from MLN and MAT by centrifuging at
148 300 g for 5 minutes (Shandon, Cheshire, UK). Slides were fixed in 100% methanol for 3
149 minutes and stained with Giemsa for 30 minutes (stain diluted 1/10 in buffered water, pH
150 7.2). Cell morphology was observed under 100x objective using an optical microscope
151 (LABORLUX S, LEITZ, Germany). 20 cells per field of view were typed as lymphocytes,
152 macrophage, eosinophils or neutrophils and percentage cell type composition of each tissue
153 was calculated. For eosinophils and neutrophils absolute cell numbers were also quantified.

154

155 2.5 Adipocyte analysis

156 MAT and SAT adipocytes were adhered to slides by cytocentrifuge at 300 g for 5 minutes
157 (Shandon, Cheshire, UK). Slides were photographed under 40x objective using UCam+
158 connected to GXCAM ECLIPSE (GT Vision, Suffolk, UK), via an objective microscope (LABORLUX
159 S, LEITZ, Germany). Absolute adipocyte cell diameters from 5 fields of view were measured
160 using image analysis software (ImageJ 1.51m9, publically available at National Institute of
161 Health), then scaled to length in μm using a graticule. Relative frequencies of cell diameters
162 were plotted per tissue.

163

164 2.6 Tissue cytokine ELISAs

165 In a separate analysis six adult beef animals were sampled at slaughter for both MLN and
166 MAT. Tissue was homogenised in PBS, supernatants were collected from homogenates after
167 centrifuging. Supernatants were tested for total protein by BCA assay and subsequently by

ELISA for IL-17A VetSet (KingFisher Biotech) and IFN-γ (MABETCH, AB, Sweden). ELISA results were expressed as ng/mg of total protein.

2.8 Statistics

All data was initially collected in Microsoft Excel and exported for graphing and statistical analysis using GraphPad Prism version 7.2 for Mac, (La Jolla, California, USA). Data are presented as mean ± SEM; statistical tests applied are indicated in the relevant figure legends and a P value of <0.05 was taken as significant. Initially data were tested for normality before application of the relevant test.

3. Results

3.1 Bovine adipose tissues possess a resident leukocyte population.

Initially, the total leukocyte cell population was estimated in the MLN, MAT, and SAT. Representative images of the major leukocytes present are presented in Figure 1A-D. Unsurprisingly in MLN there was a significantly greater pool of leukocytes compared with MAT or SAT (1637.4±104.2 $x10^5$; 16.3±2.7 $x10^5$; 11.5±1.5 $x10^5$ per g tissue in LN, MAT and SAT respectively, P<0.001) (Fig. 2). There was still however a significant difference between the total leukocyte counts of MAT and SAT ($P < 0.05$).

3.2 Compositional of leukocytes in MAT and SAT.

Leukocyte preparations were then prepared for cytospin, stained, and differential counts conducted by microscopic examination. There was a greater degree of animal to animal consistency in the MLN differential when compared to both the MAT and SAT (Figure 3A). Unsurprisingly, the MLN had the greatest proportion of lymphocytes compared to MAT and SAT but this was not significantly different (Figure 3A, 35.23%±6.13 vs 27.74%±4.0 vs 22.48%±6.3). Macrophage proportions were stable between the MLN (24.57%±4.7) and MAT (24.38±5.1) but dropped in the SAT (15.29±4.35), Figure 3A but again these were not significantly different. Eosinophils followed a different pattern where a rise in proportions was seen moving from MLN to MAT to SAT (Figure 3A; 23.88%±5.14, 39.41%±7.88, 57.45% ±9.04;2-way Anova, MLN vs MAT P<0.01, MAL vs SAT P<0.001) . This trend was clearly reversed in terms of neutrophils. With SAT having the highest proportion of neutrophils followed by MAT then MLN (Figure 3A; 16.32%±3.19, 8.47%±2.24, 4.78%±1.46; MLN vs SAT P<0.05). Despite this trend neutrophils were the smallest proportion of cells in each tissue sampled. To further examine the trend for rising neutrophil and eosinophils counts in adipose

tissues we compared the cell proportions as absolute counts. It was apparent that eosinophils numbers were greater in both adipose tissues when compared with neutrophils (Figure 3B; $P<0.05$ for SAT and $P<0.01$ for MAT).

3.3. Functional response of adipose tissue leukocytes.

To test if adipose tissues were also cytokine competent matched MLN and MAT samples from a separate cohort of animals were obtained. Levels of IFN-γ and IL-17A are presented in Figure 4A and 4B. Higher levels of both cytokines are found in the MLN compared with the matched MAT samples; statistically significant by Mann-Whitney U-Test $P<0.05$. However, it was apparent that a greater degree of variation in both cytokines was present in the MLN compared with the MAT.

3.4. Variation in adipocyte size across MAT and SAT

Adipocyte diameters (μm) were determined using ImageJ software. Thereafter adipocyte distributions were plotted (Figure 4A and 4B). MAT adipocytes have a denser frequency at a smaller diameter with a higher distribution coefficient amplitude (Gaussian distribution: amplitude = 46.06, mean = 1.115, SD = 0.2874) than SAT (Gaussian distribution: amplitude = 42.02, mean = 1.224, SD = 0.3295). This is suggestive of a smaller adipocyte cell population within the MAT depots.

4. **Discussion**

We sought to characterise the resident leukocyte population of adipose depots, we selected visceral (MAT) and subcutaneous (SAT) sites as being distinct and compared these within animals with respect to the MLN. As expected there was a larger pool of leukocytes per gram of tissue present in MLN than either type of adipose tissue. However the difference in composition between the MLN and nearest the adipose depot (MAT) was not. MAT has a profile rich in eosinophils with generous proportions of macrophage with very few neutrophils. Contrastingly, MLN is dominated by neutrophils and lymphocytes with few eosinophils. SAT had a similar leukocyte profile to that of MAT sampled here, representing a uniformity within animals. SAT was dominated by eosinophils and macrophages with low proportions of both lymphocytes and neutrophils. For both adipose depots, the proportional counts were reflected in the absolute cell counts which were dominated by eosinophils and neutrophils.

The role of adipose tissue as an endocrine organ in recent years, including functions in immunity and inflammation, has been expanded (Lehr, Hartwig and Sell, 2011). Much work has recently identified the pathways leadings from type-2 response initiation, via ILC2s andIL-25/IL-33, through to eosinophil and macrophage recruitment to adipose depots. Ultimately this drives a beiging process with upregulated UCP1 expression and a transition of WAT to BAT. This process can be initiated either by injection of the canonical type-2 cytokines IL-25 or IL-33, or by nematode infection. Considering the mechanisms indicating eosinophils ultimately promote beiging of adipose tissue (Qiu et al., 2014), we may expect to see a greater proportion of BAT over WAT in the eosinophil rich MAT and SAT. Work by Lapa et al. (2017) showed a smaller adipocyte diameter is associated with BAT cells. While there was both a difference in the range of adipocyte diameters from our adipose depots and eosinophil counts

there was no significant difference between either of these parameters. On the contrary, mean adipocyte diameter of SAT is larger than that of MAT however the range of diameters for SAT is larger. It may be possible that this range occurs from the presence of a variety of WAT and BAT as more adipocyte precursors are stimulated to beige here, whereas the visceral nature of MAT predisposes it to smaller adipocyte size and a BAT driven thermogenesis function (Hocking et al., 2010).

Functional testing of the adipose resident leukocytes suggested that the MAT depot, was competent in terms of IL-17A and IFN-γ production. For both cytokines however, the MLN produced greater amounts compared with the MAT. Strikingly, there was larger animal to animal variation for both cytokines within the MLN compared with the MAT; this may be reflective of the reactive nature of the MLN. Ultimately, our findings demonstrate that cellular sources of two major T-helper cytokines are present within MAT tissue. . Individual variation between animals of IFNγ production could be rationalised by recent findings that WAT is enriched with memory CD8 T-cells, serving as a pool of anti-microbial effectors (Han et al., 2017). A detailed investigation of the T-cell phenotypes will be required to fully understand the nature of the interaction between potential IFN-γ producing lymphocytes and resident eosinophils. The link between non-specific inflammation and obesity has long been established. Gomez-Ambrosi et al., (2002) established a relationship between high leptin levels in obese patients. Moreover, leptin was also correlated with C-reactive protein, linking inflammation and obesity. The dynamic nature of this relationship was proven when obese patients undergoing weight loss surgery were shown to have reduced SAA levels compared to their pre-surgery levels (Gomez-Ambrosi et al., 2006). Alongside the changes in SAA there was also a notable leptin decrease in the same cohort of patients, demonstrating that the inflammatory state may be driven in part by leptin. Previously, Worthington et al., (2013) had

shown that high leptin impaired the murine type-2 response to nematode infection delaying worm expulsion. Thus obesity-linked inflammation (type-1 or type-17 responses) can diminish the type-2 response. Mouse models showing a lean phenotype in IL-1Rα (Hirsch et al., PNAS 1996) and TNF-α (Ventre et al., Diabetes 1997). support the role for baseline homeostatic inflammation in maintaining adipose tissue.

The immune-adipose pathway has already been clinically targeted in ruminants. Goats administered 2,4-thiazolidinedione (TZD) – a PPARGγ agonist – had improved somatic cells counts in milk and reduced inflammatory markers (Rosa et al., 2017). Understanding the mechanisms behind this causal relationship and the associations identified above could provide novel therapeutics to improve animal production. Applying the data from this study now provides opportunities to evaluate whether or not differences are observed in adipose tissue composition and immune system activity, under routine challenges such as parasitic infection and dietary constraints or resource restriction.

Acknowledgments

We would like to thank participating premises for access to tissues and Dr Parul Sharma and Paul Gilmore for assistance with laboratory work. This work was completed as partial fulfilment for an MRes (Clinical Sciences) award to EB.

297

298 **References**

299 Azeez, O., Meintjes, R. and Chamunorwa, J. (2014). Adipose tissue body, adipose tissue pad
300 and adipose tissues in invertebrates and vertebrates: the nexus. *Lipids in Health and*
301 *Disease*, 13(1), p.71.

302 Cannon, B. and Nedergaard, J. (2004). Brown Adipose Tissue: Function and Physiological
303 Significance. *Physiological Reviews*, 84(1), pp.277-359.

304 Gómez-Ambrosi, J., Salvador, J., Páramo, J.A., Orbe, J., de Irala, J., Diez-Caballero, A., Gil,
305 M.J., Cienfuegos, J.A. and Frühbeck, G. (2002). Involvement of leptin in the
306 association between percentage of body fat and cardiovascular risk factors. *Clinical*
307 *Biochemistry*, 35(4), pp.315-320.

308 Gómez-Ambrosi, J., Salvador, J., Rotellar, F., Silva, C., Catalán, V., Rodríguez, A., Jesús Gil, M.
309 and Frühbeck, G. (2006). Increased serum amyloid A concentrations in morbid
310 obesity decrease after gastric bypass. *Obesity Surgery*, 16(3), pp.262-269.

311 Han, S., Glatman Zaretsky, A., Andrade-Oliveira, V., Collins, N., Dzutsev, A., Shaik, J., Morais
312 da Fonseca, D., Harrison, O., Tamoutounour, S., Byrd, A., Smelkinson, M., Bouladoux, N.,
313 Bliska, J., Brenchley, J., Brodsky, I. and Belkaid, Y. (2017). White Adipose Tissue Is a
314 Reservoir for Memory T Cells and Promotes Protective Memory Responses to
315 Infection. *Immunity*, 47(6), pp.1154-1168.e6.

316 Hocking, S., Wu, L., Guilhaus, M., Chisholm, D. and James, D. (2010). Intrinsic Depot-Specific
317 Differences in the Secretome of Adipose Tissue, Preadipocytes, and Adipose Tissue-
318 Derived Microvascular Endothelial Cells. *Diabetes*, 59(12), pp.3008-3016.

Hirsch, E., Irikura, V.M., Paul, S.M. and Hirsh, D. (1996). Functions of interleukin 1 receptor antagonist in gene knockout and overproducing mice. *Proceedings of the National Academy of the Sciences of the United States of America*, 93(20), pp11008-11013.

Johnson, D., Hayward, J., Jacobs, T., Collis, M., Eckerson, J. and Williams, R. (1977). Plasma norepinephrine responses of man in cold water. *Journal of Applied Physiology*, 43(2), pp.216-220.

Kae Won Cho, David L. Morris, Carey N. Lumeng, Chapter Sixteen - Flow Cytometry Analyses of Adipose Tissue Macrophages, Editor(s): Ormond A. Macdougald, Methods in Enzymology, Academic Press, Volume 537, 2014, Pages 297-314

Lapa, C., Arias-Loza, P., Hayakawa, N., Wakabayashi, H., Werner, R., Chen, X., Shinaji, T., Herrmann, K., Pelzer, T. and Higuchi, T. (2017). Whitening and Impaired Glucose Utilization of Brown Adipose Tissue in a Rat Model of Type 2 Diabetes Mellitus. *Scientific Reports*, 7(1).

Lee, M., Odegaard, J., Mukundan, L., Qiu, Y., Molofsky, A., Nussbaum, J., Yun, K., Locksley, R. and Chawla, A. (2015). Activated Type 2 Innate Lymphoid Cells Regulate Beige Adipose tissue Biogenesis. *Cell*, 160(1-2), pp.74-87.

Lehr, S., Hartwig, S. and Sell, H. (2011). Adipokines: A treasure trove for the discovery of biomarkers for metabolic disorders. *PROTEOMICS - Clinical Applications*, 6(1-2), pp.91-101.

Molofsky, A., Nussbaum, J., Liang, H., Van Dyken, S., Cheng, L., Mohapatra, A., Chawla, A. and Locksley, R. (2013). Innate lymphoid type 2 cells sustain visceral adipose tissue eosinophils and alternatively activated macrophages. *The Journal of Experimental Medicine*, 210(3), pp.535-549.

342 Nguyen, K., Qiu, Y., Cui, X., Goh, Y., Mwangi, J., David, T., Mukundan, L., Brombacher, F.,
343 Locksley, R. and Chawla, A. (2011). Alternatively activated macrophages produce
344 catecholamines to sustain adaptive thermogenesis. *Nature*, 480(7375), pp.104-108.
345 Nussbaum, J., Van Dyken, S., von Moltke, J., Cheng, L., Mohapatra, A., Molofsky, A., Thornton,
346 E., Krummel, M., Chawla, A., Liang, H. and Locksley, R. (2013). Type 2 innate lymphoid
347 cells control eosinophil homeostasis. *Nature*, 502(7470), pp.245-248.
348 Odegaard, J., Lee, M., Sogawa, Y., Bertholet, A., Locksley, R., Weinberg, D., Kirichok, Y., Deo,
349 R. and Chawla, A. (2016). Perinatal Licensing of Thermogenesis by IL-33 and ST2. *Cell*,
350 166(4), pp.841-854.
351 Odegaard, J., Ricardo-Gonzalez, R., Goforth, M., Morel, C., Subramanian, V., Mukundan, L.,
352 Eagle, A., Vats, D., Brombacher, F., Ferrante, A. and Chawla, A. (2007). Macrophage-
353 specific PPARγ controls alternative activation and improves insulin resistance. *Nature*,
354 447(7148), pp.1116-1120.
355 Pope, M., Budge, H. and Symonds, M. (2013). The developmental transition of ovine adipose
356 tissue through early life. *Acta Physiologica*, 210(1), pp.20-30.
357 Qiu, Y., Nguyen, K., Odegaard, J., Cui, X., Tian, X., Locksley, R., Palmiter, R. and Chawla, A.
358 (2014). Eosinophils and Type 2 Cytokine Signaling in Macrophages Orchestrate
359 Development of Functional Beige Adipose tissue. *Cell*, 157(6), pp.1292-1308.
360 Restelli, L., Codrea, M., Savoini, G., Ceciliani, F. and Bendixen, E. (2014). LC-MS/MS analysis of
361 visceral and subcutaneous adipose tissue proteomes in young goats with focus on innate
362 immunity and inflammation related proteins. *Journal of Proteomics*, 108, pp.295-305.
363 Rosa, F., Osorio, J., Trevisi, E., Yanqui-Rivera, F., Estill, C. and Bionaz, M. (2017). 2,4-
364 Thiazolidinedione Treatment Improves the Innate Immune Response in Dairy Goats with
365 Induced Subclinical Mastitis. *PPAR Research*, 2017, pp.1-22.

Smith, S., Carstens, G., Randel, R., Mersmann, H. and Lunt, D. (2004). Brown adipose tissue development and metabolism in ruminants. *Journal of Animal Science*, 82(3), p.942.

Teixeira, L., Moreira, J., Melo, J., Bezerra, F., Marques, R., Ferreirinha, P., Correia, A., Monteiro, M., Ferreira, P. and Vilanova, M. (2015). Immune response in the adipose tissue of lean mice infected with the protozoan parasite Neospora caninum. *Immunology*, 145(2), pp.242-257.

Ventre, J., Doebber, T., Wu, M., MacNaul, K., Stevens, K., Pasparakis, M., Kollias, G. and Moller, D.E. (1997). Targeted disruption of the tumor necrosis factor-alpha gene: metabolic consequences in obese and nonobese mice. *Diabetes*, 46(9), pp.1526-1531.

Wilhelm, C., Harrison, O., Schmitt, V., Pelletier, M., Spencer, S., Urban, J., Ploch, M., Ramalingam, T., Siegel, R. and Belkaid, Y. (2016). Critical role of adipose tissuety acid metabolism in ILC2-mediated barrier protection during malnutrition and helminth infection. *The Journal of Experimental Medicine*, 213(8), pp.1409-1418.

Worthington, J.J., Samuelson, L.C., Grencis, R.K. and McLaughlin, J.T. (2013). Adaptive immunity alters distinct host feeding pathways during nematode induced inflammation, a novel mechanism in parasite expulsion. *PLoS Pathogens*, 9(1): e1003122.

Wu, D., Molofsky, A., Liang, H., Ricardo-Gonzalez, R., Jouihan, H., Bando, J., Chawla, A. and Locksley, R. (2011). Eosinophils Sustain Adipose Alternatively Activated Macrophages Associated with Glucose Homeostasis. *Science*, 332(6026), pp.243-247.

Figure Legends:

Figure 1: Representative leukocytes. Giemsa stained leukocytes isolated from bovine MAT or SAT, representative of cells identified in differential cell counting. Images were captured via Zen on a Zeiss Imager M2AX10 (Oberkochen, Germany). Scale bar 10 μm is shown in images; A – macrophage (arrowhead) and lymphocyte (arrow); B – eosinophil (arrowhead); C - neutrophil (arrowhead).

Figure 2: Adipose tissue leukocytes. Total Leukocyte cell counts for MLN (N=9), MAT (N=10) and SAT (N=10) as expressed as cells ($x10^5$)/g tissue. Individual data is presented with means ±SEM. Data were analysed by Kruskal-Wallis test with Dunns multiple comparisons test. MLN was significantly different compared to both MAT and SAT ($P<0.001$), with MAT vs SAT differences ($P<0.05$).

Figure 2: Adipose tissue leukocyte composition. (A) Differential counts were performed on cytospins from (N=8) animals for each tissue type with at least 5 fields of view, containing 20 cells, per slide. Differences between cell type and tissue were tested via 2-way Anova where *$P<0.05$ and ** $P<0.001$. (B) Absolute cell numbers for eosinophils and neutrophils were calculated and presented as 10^5 cells/g tissue. Differences between cell type and tissue were tested via 2-way Anova where *$P<0.05$ and ** $P<0.001$.

Figure 4: Adipose tissue cytokine levels. Matched MLN and MAT tissues (N=6) were homogenised and tested for IFN-γ (A) and IL-17A (B). Cytokine levels are presented as ng (of cytokine) per mg of total protein. Differences amongst tissues were tested by Mann-Whitney Test (* $P<0.05$).

Figure 5: Adipocyte parameters within MAT and SAT. (A) Frequency distribution of the diameter of adipocytes (μm) isolated from MAT, n=684. Gaussian distribution curve is plotted (amplitude = 46.06, mean = 1.115, SD = 0.2874). (B) Frequency distribution of the diameter

414 of adipocytes (μm) isolated from SAT, n=738. Gaussian distribution curve is plotted

415 (amplitude = 42.02, mean = 1.224, SD = 0.3295).

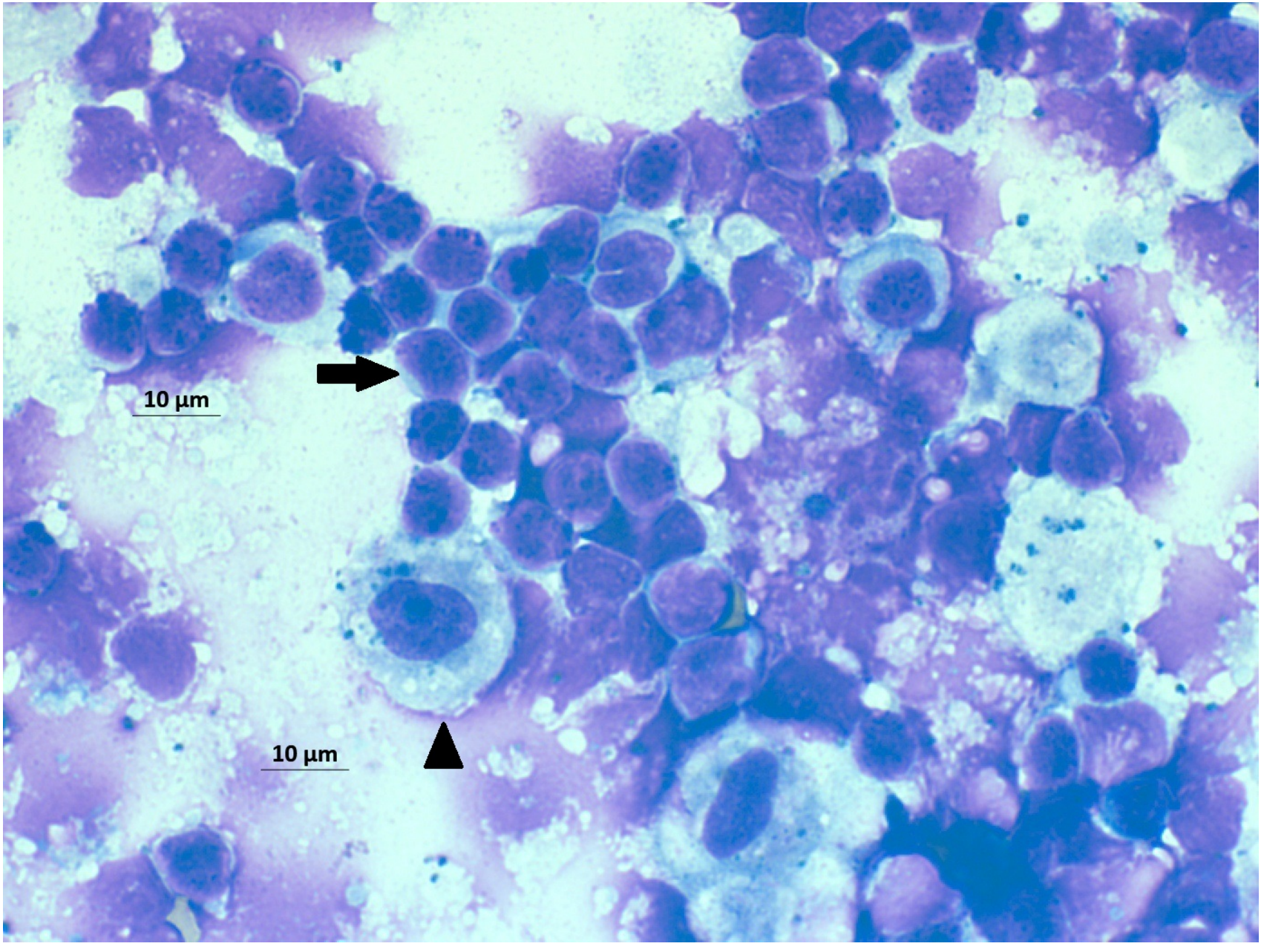
10 µm
10 µm

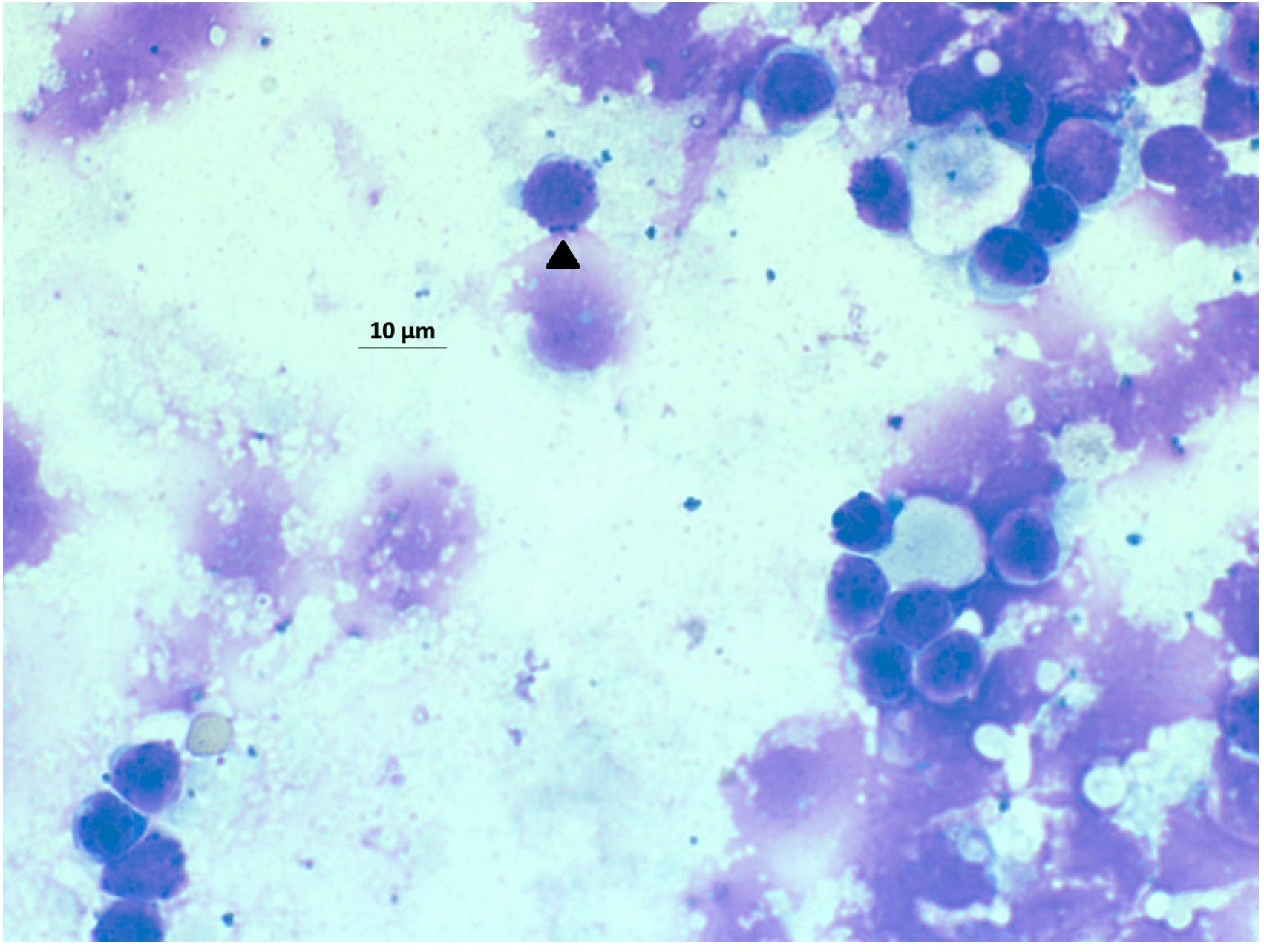
10 µm

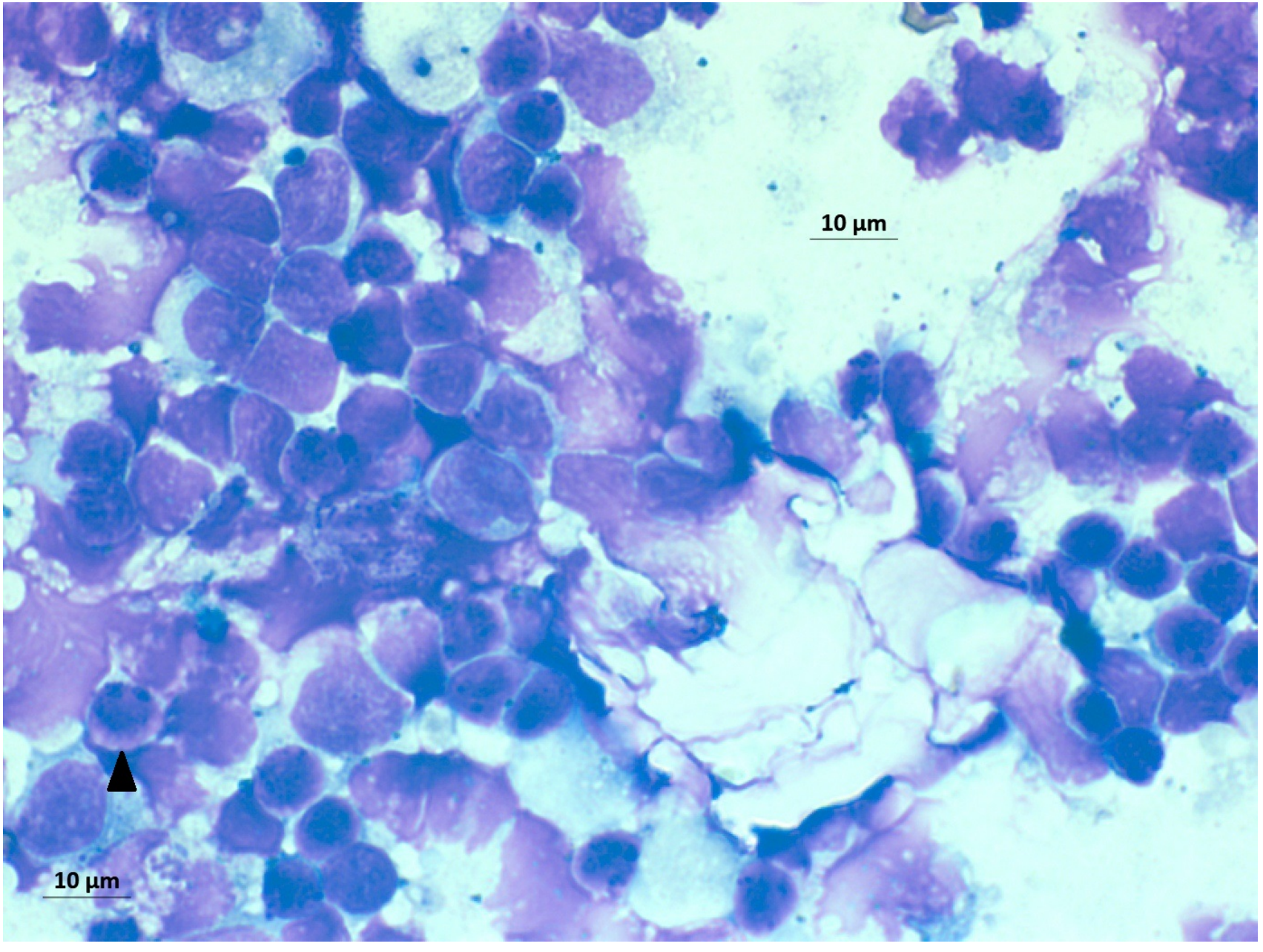
10 µm
10 µm

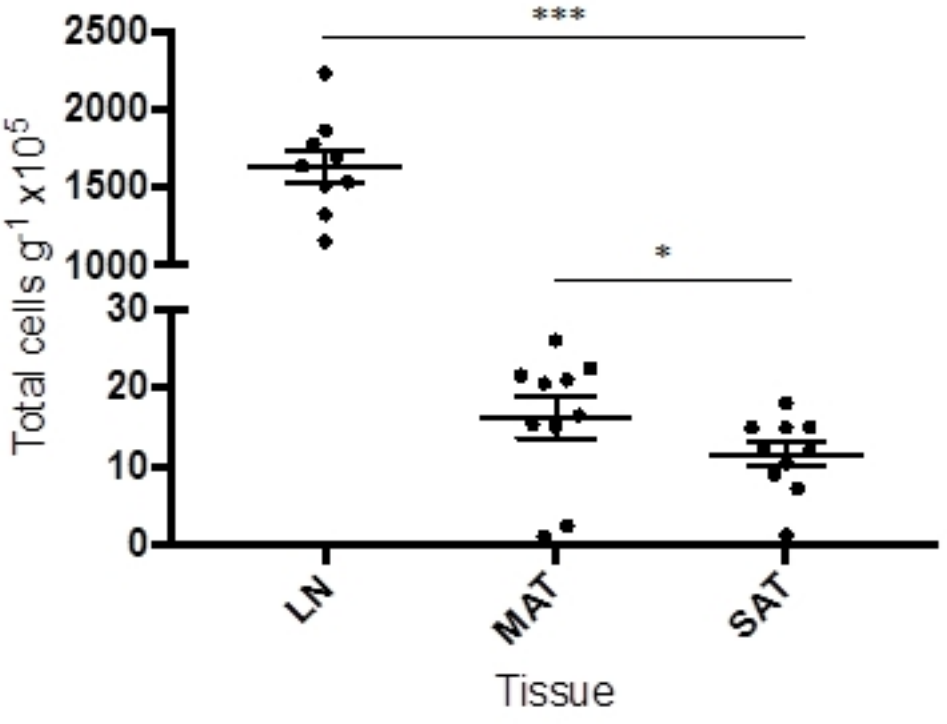
***
*
2500
2000
1500
1000
30
20
10
0
Total cells g-1 x105
LN
MAT
SAT
Tissue

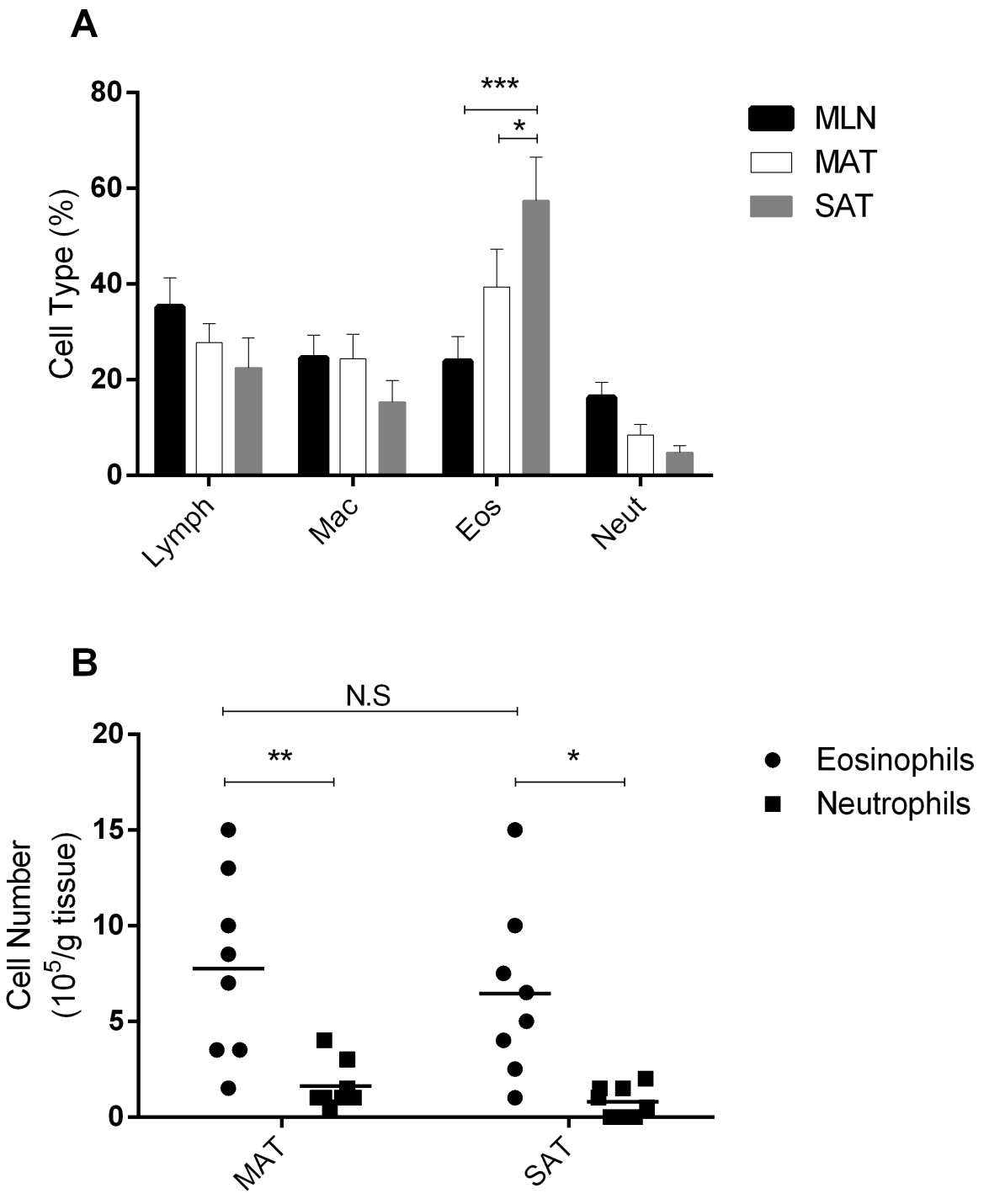
A
80
60
40
20
0
Cell Type (%)
***
*
MLN
MAT
SAT
Lymph
Mac
Eos
Neut
B
N.S
**
*
20
15
10
5
0
Cell Number
(10^5/g tissue)
Eosinophils
Neutrophils
MAT
SAT

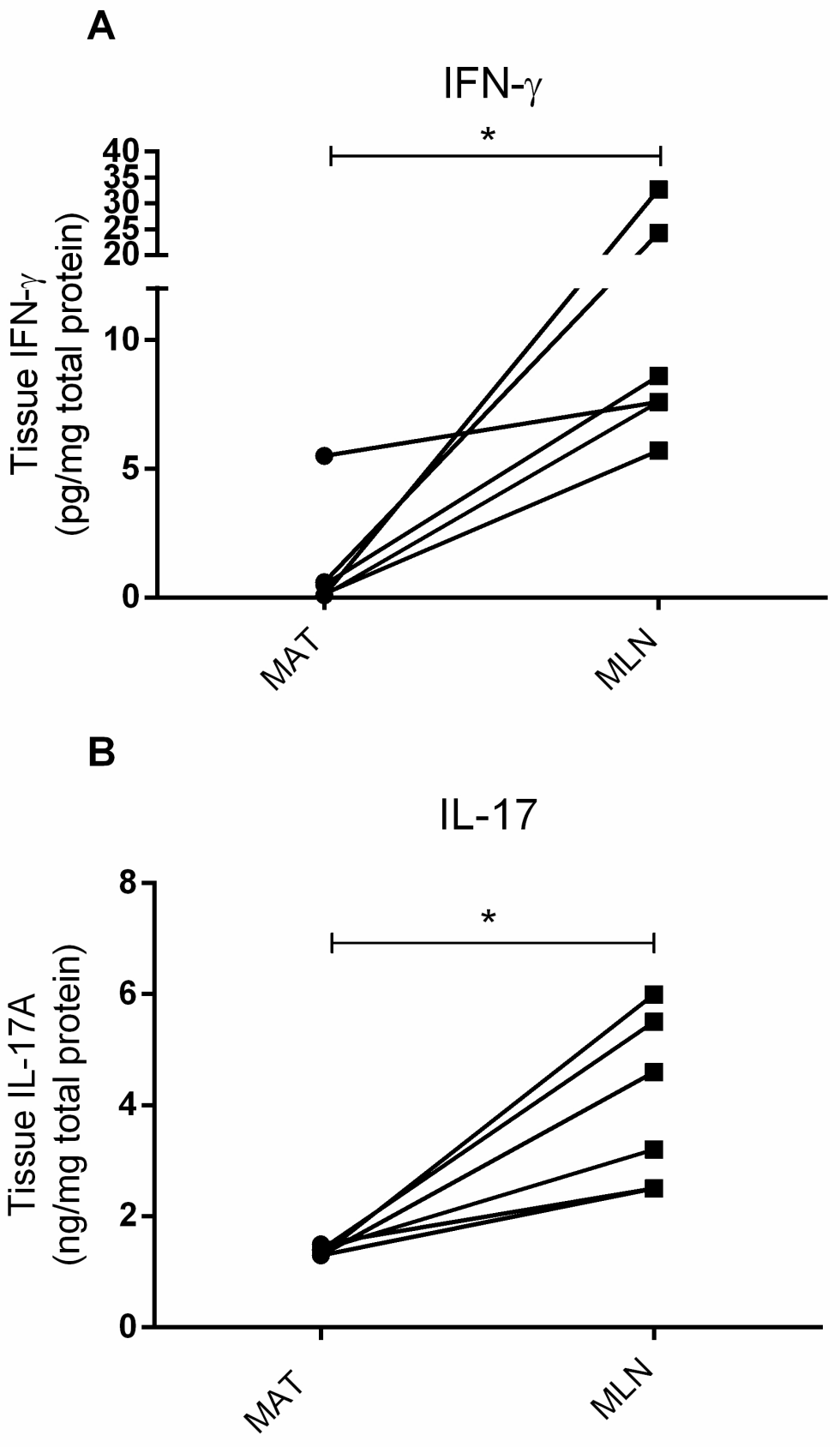
A
IFN-γ
*
40
35
30
25
20
10
5
0
Tissue IFN-γ
(pg/mg total protein)
MAT
MLN
B
IL-17
*
8
6
4
2
0
Tissue IL-17A
(ng/mg total protein)
MAT
MLN

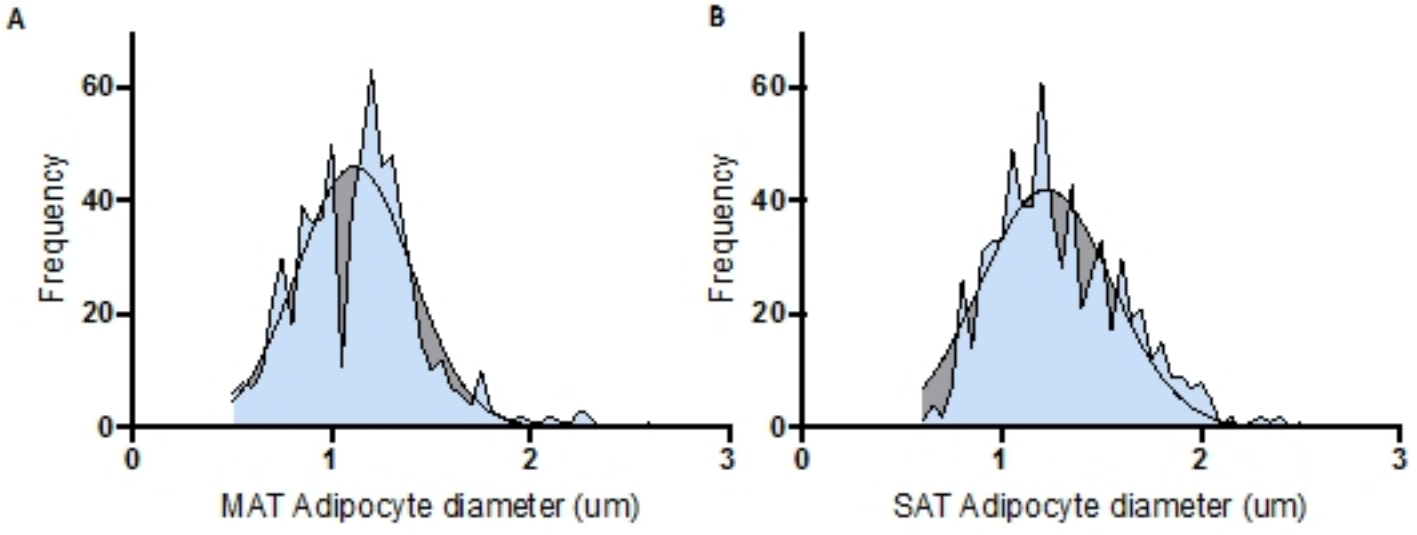
A
Frequency
60
40
20
0
0
1
2
3
MAT Adipocyte diameter (um)
B
Frequency
60
40
20
0
0
1
2
3
SAT Adipocyte diameter (um)